

Supporting information

Experimental details

X-ray data collections and structural determinations.

Diffraction data for crystals of the nickel(II)-chlorido complex with $\text{Tp}^{\text{Me}_2,\text{Br}}$ derived from toluene ($= \mathbf{3}^{\text{Br}} \cdot 0.5\text{toluene}$) and an EtOH adduct of the nickel(II)-*m*CBA complex with $\text{Tp}^{\text{Me}_2,\text{Br}}$ derived from EtOH ($= \mathbf{4}^{\text{Br}}(\text{EtOH})_2$) were collected using a Rigaku Satarn 70 CDD area detector system with graphite monochromated Mo-K α radiation. The crystals were mounted on loops using liquid paraffin flash cooled to 113 K and the data collections were carried at the same temperature. Diffraction measurement of the nickel(II)-*m*CBA complex with Tp^{iPr_2} derived from pentane ($= \mathbf{4}'^{\text{H}}$) was made on a Rigaku RAXIS IV imaging plate area detector with Mo K α radiation. The crystal was mounted on glass fiber and data collection was carried out at 213 K.

Crystallographic data and the result of refinement are summarized in Table S-1. Structure analyses were performed by using Win-GX program package.¹ The structures of the complexes were solved by the direct methods using SIR-92 program.² The structures were refined on F^2 with full-matrix least-squares methods using SHELXL-97.^{3,4} All non-hydrogen atoms except the carbon atoms of a disordered toluene molecule were refined anisotropically. Hydrogen atoms on the pyrazoly and phenyl groups were added in the riding model with C–H = 0.96 Å (for methyl groups), 0.98 Å (for methine groups) or 0.93 Å (for aromatic rings) with $U_{\text{iso}}(\text{H}) = 1.2 U_{\text{iso}}(\text{attached atom})$. Hydrogen atoms attached on the boron centers of Tp^{R} and on the oxygen atoms of EtOH were refined isotropically. CCDC 874059 ($\mathbf{3}^{\text{Br}} \cdot 0.5\text{toluene}$), CCDC 874060 ($\mathbf{4}^{\text{Br}}(\text{EtOH})_2$), and CCDC 163522 ($\mathbf{4}'^{\text{H}}$) contain the supplementary crystallographic data for this paper. The deposited data can be obtained free of charge from The Cambridge Crystallographic Data Centre via www.ccdc.cam.ac.uk/data_request/cif.

References for supporting information

- 1 L. J. Farrugia, *J. Appl. Crystallogr.*, 1999, **32**, 837–838.
- 2 A. Altomare, M. C. Burla, M. Camalli, M. Cascarano, C. Giacovazzo, A. Guagliardi and G. Polidori, *J. Appl. Crystallogr.*, 1994, **27**, 435–436.
- 3 G. M. Sheldrick, SHELXL-97, University of Göttingen, Germany, 1997.
- 4 G. M. Sheldrick, *Acta. Crystallogr.*, 2008, **A64**, 112–122.

Table S1 Crystallographic data

	3^{Br}·0.5toluene	4^{Br}(EtOH)₂	4'^H
Formula	C _{16.5} H ₂₃ BBr ₃ ClN ₆ Ni	C ₂₆ H ₃₅ BBr ₃ ClN ₆ NiO ₄	C ₃₄ H ₅₀ BClN ₆ NiO ₂
Formula weight	674.13	840.30	679.77
Crystal system	Monoclinic	Triclinic	Monoclinic
Space group	P2 ₁ /a (#14)	P ₁ (#2)	P2 ₁ /n (#14)
a/Å	10.8874(14)	10.897(5)	12.3257(10)
b/Å	19.586(3)	11.565(5)	18.8319(16)
c/Å	12.2781(16)	14.060(5)	15.697(2)
α/°	90	78.696(5)	90
β/°	90.982(4)	71.796(5)	95.5920(10)
γ/°	90	82.924(5)	90
V/Å ³	2617.8(6)	1646.9(12)	3626.1(6)
Z	4	2	4
D (calc.)/g cm ⁻³	1.710	1.695	1.245
μ(Mo-Kα)/mm ⁻¹	5.440	4.350	0.646
Unique reflections	5921	6621	7240
Reflections $I > 2\sigma(I)$	5720	6434	5422
Parameters refined	260	399	419
R ($I > 2\sigma(I)$)	0.0552	0.0340	0.0513
R (for all data)	0.0570	0.0350	0.0722
wR ($I > 2\sigma(I)$)	0.1423	0.0899	0.1319
wR (for all data)	0.1444	0.0909	0.1391
GOF	1.115	1.107	1.044

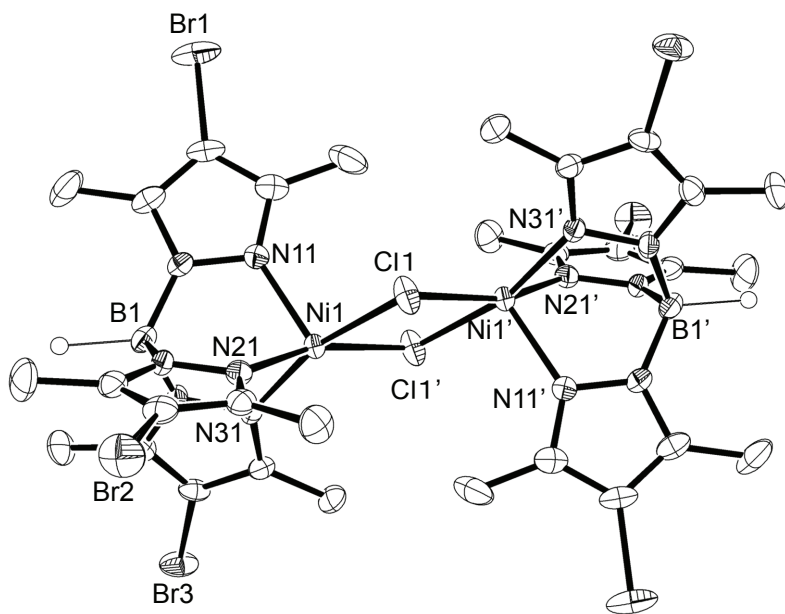


Fig. S1 Dimeric structure of $\mathbf{3}^{\text{Br}}$ drawn at the 30% probability level. All hydrogen atoms except boron-bounded ones on $\text{Tp}^{\text{Me}2,\text{Br}}$ are omitted for clarity. The analyzed crystals obtained from a toluene solution exhibited green color due to five-coordinated nickel(II) centers. However, $\mathbf{3}^{\text{Br}}$ had a monomeric structure with pseudo-tetrahedral nickel(II) center in the non-coordinating solvent such as toluene and CH_2Cl_2 as was supported by reddish brown solution color similar to that of the previously reported tetrahedral nickel(II)-bromido complex with $\text{Tp}^{\text{Me}2}$, namely $[\text{Ni}^{\text{II}}(\text{Br})(\text{Tp}^{\text{Me}2})]$ (P. J. Desrochers, J. Telser, S. A. Zvyagin, A. Ozarowski, J. Krzystek and D. A. Vicic, *Inorg. Chem.*, 2006, **45**, 8930 – 8941).

Table S2 Selected bond lengths (\AA) and angles(deg) for $\mathbf{3}^{\text{Br}} \cdot 0.5\text{toluene}$.

Lengths (\AA)			
Ni1–N11	2.011(3)	Ni1–N21	2.063(3)
Ni1–N31	2.061(3)	Ni1–Cl1	2.3792(11)
Ni1–Cl1'	2.3611(11)	Ni1···Ni1'	3.5415(10)
Angles (deg)			
N11–Ni1–N21	92.28(14)	N11–Ni1–N31	92.16(13)
N11–Ni1–Cl1	101.91(11)	N11–Ni1–Cl1'	104.84(11)
N21–Ni1–N31	86.99(13)	N21–Ni1–Cl1	92.07(9)
N21–Ni1–Cl1'	162.83(10)	N31–Ni1–Cl1	165.93(10)
N31–Ni1–Cl1'	93.48(9)	Cl1–Ni1–Cl1'	83.32(4)

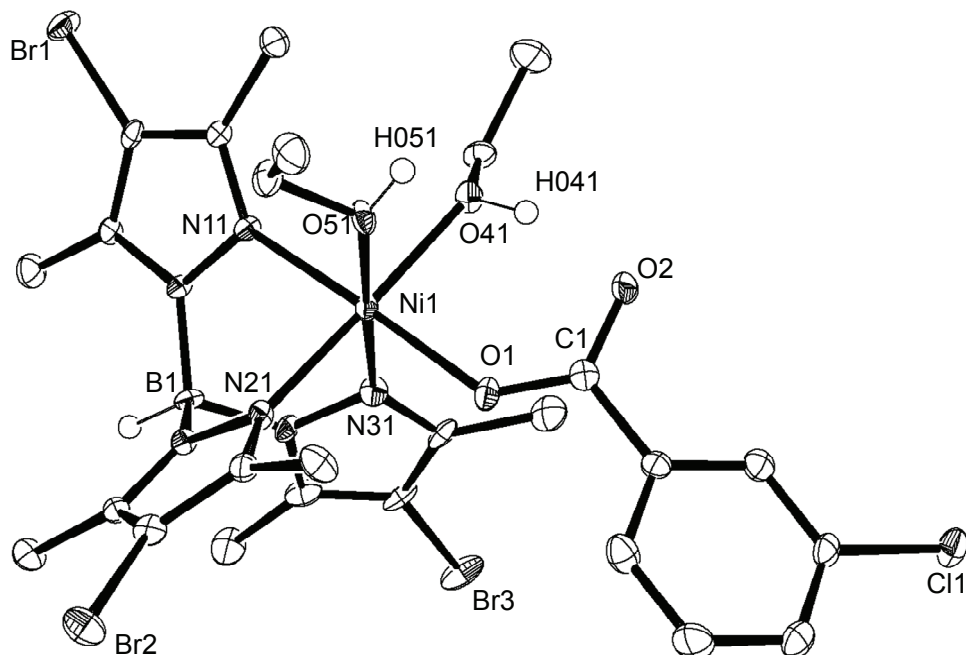


Fig. S2 Molecular structure of $\mathbf{4}^{\text{Br}}(\text{EtOH})_2$ drawn at the 30% probability level. Hydrogen atoms except those attached on the oxygen atoms of the coordinated EtOH molecules (i.e. O41 and O51) and the boron of $\text{Tp}^{\text{Me}_2,\text{Br}}$ (i.e. B1) are omitted for clarity.

Table S3 Selected bond lengths (\AA) and angles(deg) for $\mathbf{4}^{\text{Br}}(\text{EtOH})_2$.

Lengths (\AA)			
Ni1–N11	2.092(2)	Ni1–N21	2.086(2)
Ni1–N31	2.092(2)	Ni1–O1	2.3792(11)
Ni1–O41	2.0838(18)	Ni1–O51	2.1209(18)
Angles (deg)			
N11–Ni1–N21	89.26(8)	N11–Ni1–N31	88.17(8)
N11–Ni1–O1	177.89(7)	N11–Ni1–O41	91.96(8)
N11–Ni1–O51	94.03(8)	N21–Ni1–N31	88.97(8)
N21–Ni1–O1	89.05(8)	N21–Ni1–O41	174.02(7)
N21–Ni1–O51	90.65(8)	N31–Ni1–O1	90.53(8)
N31–Ni1–O41	96.91(8)	N31–Ni1–O51	177.77(8)
O1–Ni1–O41	89.85(7)	O1–Ni1–O51	87.26(8)
O41–Ni1–O51	83.42(7)		

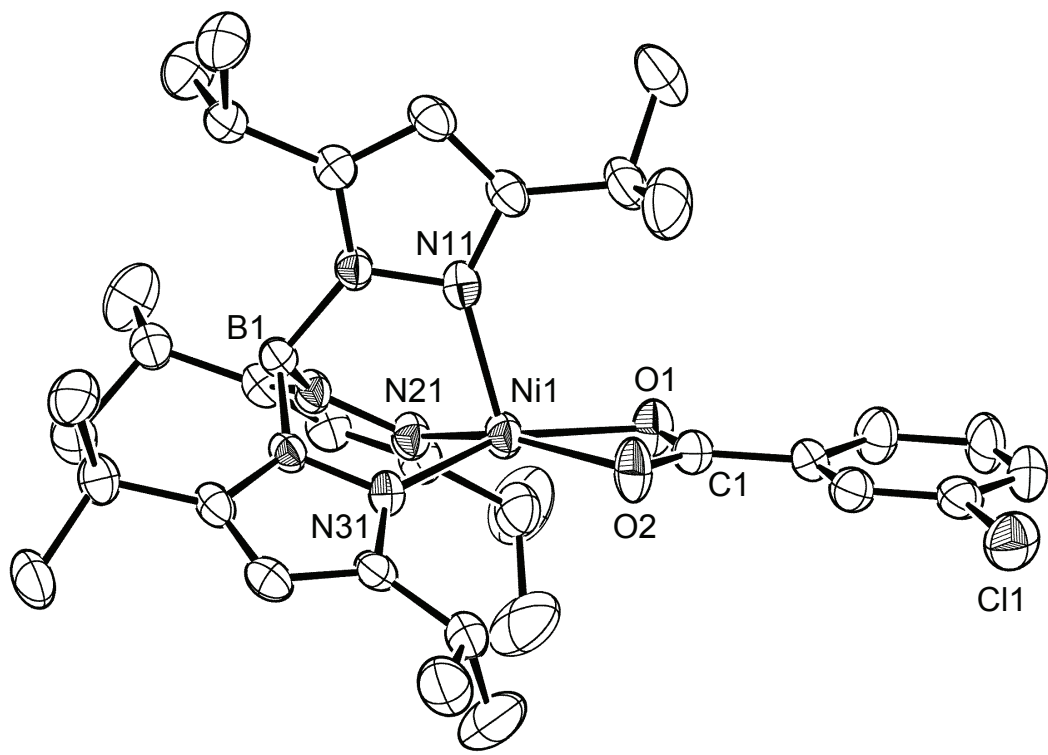


Fig. S3 Molecular structure of 4^{H} drawn at the 30% probability level. All hydrogen atoms are omitted for clarity.

Table S4 Selected bond lengths (\AA) and angles(deg) for 4^{H} .

Lengths (\AA)			
Ni1–N11	2.012(2)	Ni1–N21	2.011(2)
Ni1–N31	2.015(2)	Ni1–O1	2.0908(18)
Ni1–O2	2.085(2)		
Angles (deg)			
N11–Ni1–N21	90.19(9)	N11–Ni1–N31	92.51(8)
N11–Ni1–O1	106.20(8)	N11–Ni1–O2	107.34(9)
N21–Ni1–N31	92.06(9)	N21–Ni1–O1	100.41(8)
N21–Ni1–O2	158.32(8)	N31–Ni1–O1	157.32(9)
N31–Ni1–O2	99.62(8)	O1–Ni1–O2	63.00(7)

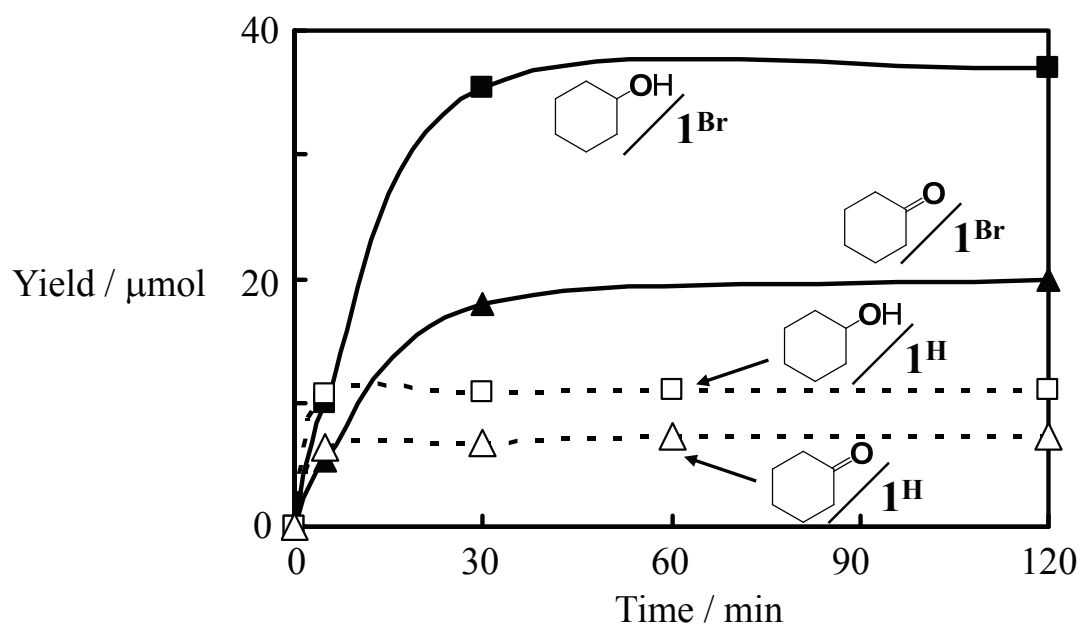
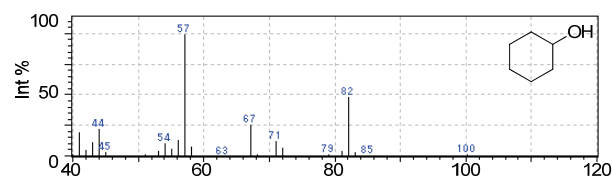


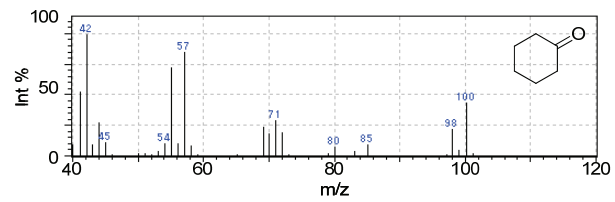
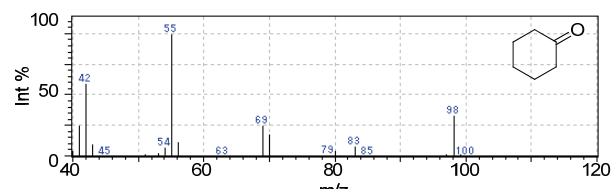
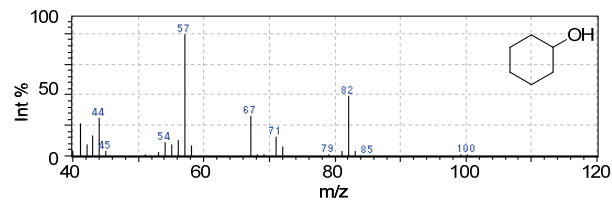
Fig. S4 Time course of the oxygenation of cyclohexane with mCPBA mediated by $\mathbf{1}^{\mathbf{X}}$ ($\mathbf{X} = \mathbf{H}, \mathbf{Br}$) in $\text{CF}_3\text{C}_6\text{H}_5$. Conditions: $[\mathbf{1}^{\mathbf{X}}] = 5.2 \text{ mM}$ in 5 mL of $\text{C}_6\text{H}_5\text{CF}_3$, Ni: mCPBA: $\text{C}_6\text{H}_{12} = 1:5:50$, at 313 K, under argon.

(a) Reaction mediated by $\mathbf{1}^{\mathbf{H}}$

H_2^{16}O (control)

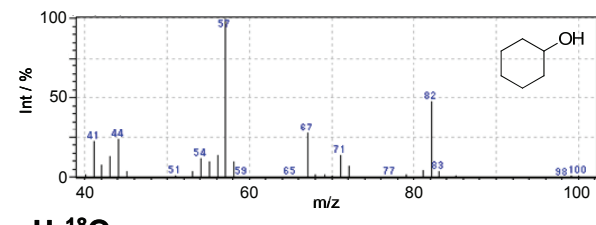


H_2^{18}O



(b) Reaction mediated by $\mathbf{1}^{\mathbf{Br}}$

H_2^{16}O (control)



H_2^{18}O

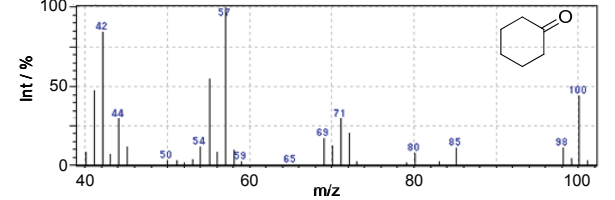
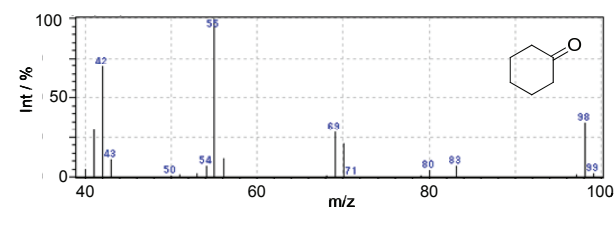
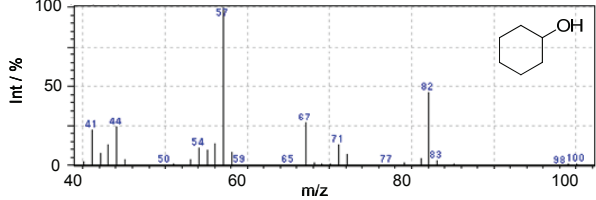


Fig. S5 GC-MS spectra of the products obtained by oxygenation of cyclohexane with *m*CPBA mediated by $\mathbf{1}^{\mathbf{X}}$ in the presence of H_2^{18}O . Reactions in the presence of H_2^{16}O were also examined as control. Conditions: $[\mathbf{1}^{\mathbf{X}}] = 2.6 \text{ mM}$ in 1 mL of CH_2Cl_2 , $\text{Ni:mCPBA:H}_2\text{O:C}_6\text{H}_{12} = 1:50:500:2500$, at 313 K, under argon. In a mass spectrum of cyclohexanol products, any signals attributed to the ^{18}O -incorporated compounds could not be detected. In the spectra of cyclohexanone, a peak at $m/z = 100$ could be assigned as ^{18}O -cyclohexanone.

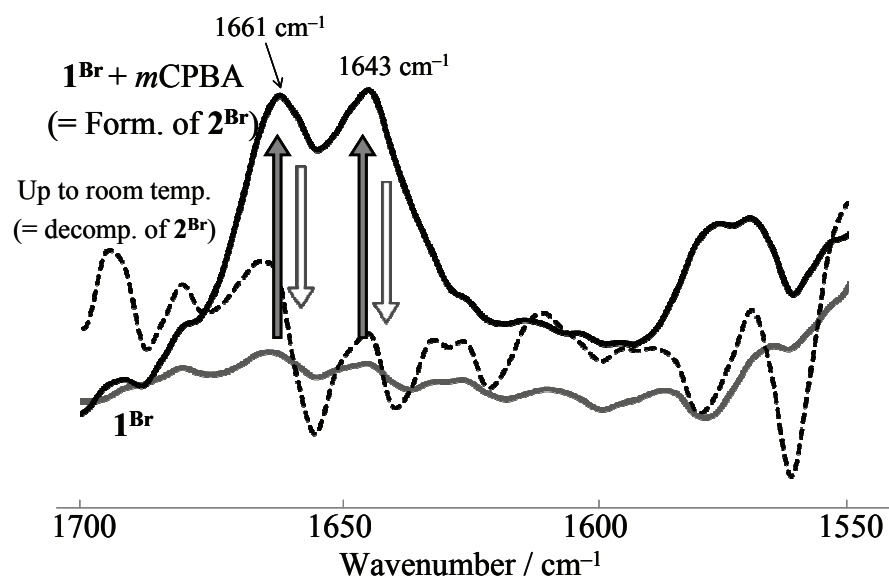


Fig. S6 IR spectra of the CH_2Cl_2 solutions of *in situ* generated $\mathbf{2}^{\text{Br}}$ (formed by the reaction of $\mathbf{1}^{\text{Br}}$ with 2 equiv of *m*CPBA; top; black line), the parent $\mathbf{1}^{\text{Br}}$ (bottom; gray line), and the sample once wormed up to room temperature (recorded at 223 K; dashed line). Both peaks at 1661 and 1643 cm^{-1} disappeared by warm up of the solution. Therefore, we assigned the both peaks were attributed to the $\nu\text{C=O}$ bands of the thermally unstable nickel(II)-acylperoxo species $\mathbf{2}^{\text{Br}}$, and one of two peaks might attribute to an aqua ligand adduct of $\mathbf{2}^{\text{Br}}$.

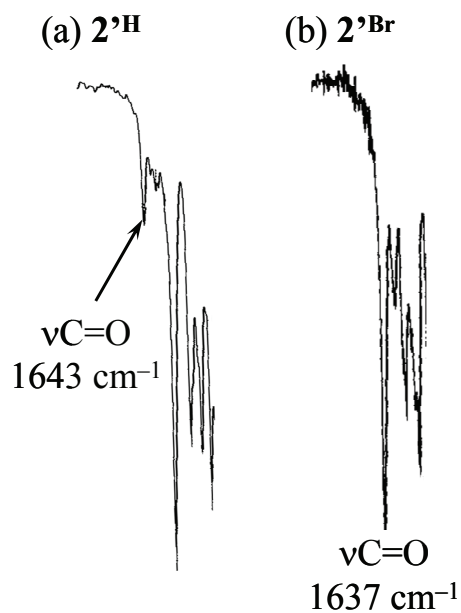


Fig. S7 IR spectra of the KBr pellet samples of $\mathbf{2}^{\text{H}}$ (a; left) and $\mathbf{2}^{\text{Br}}$ (b; right).

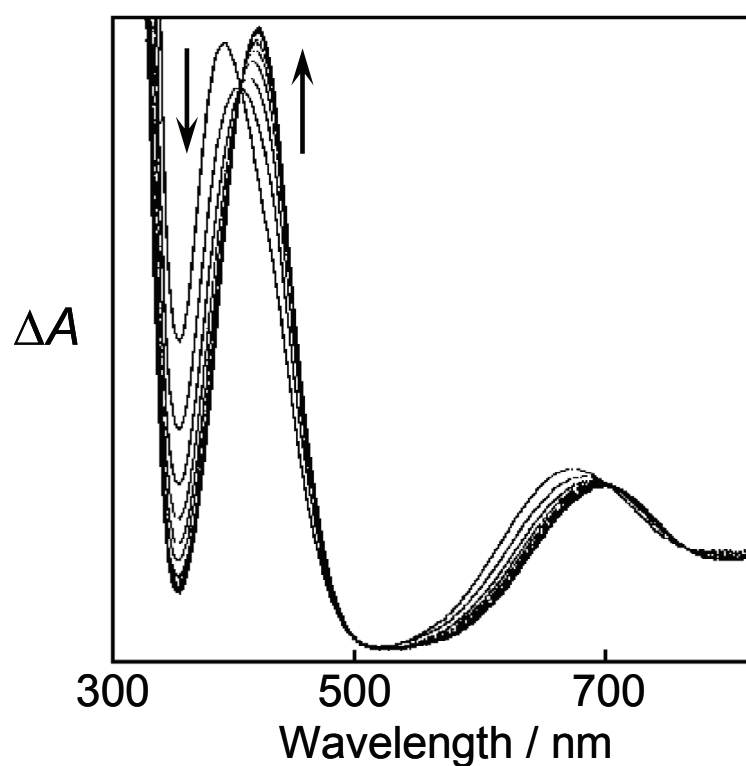


Fig. S8 Decay of 2^{H} in Et_2O observed by time course UV/Vis spectra. Increasing absorbance at 429 nm indicated the formation of the mCBA complexes 4^{H} and 5^{H} .

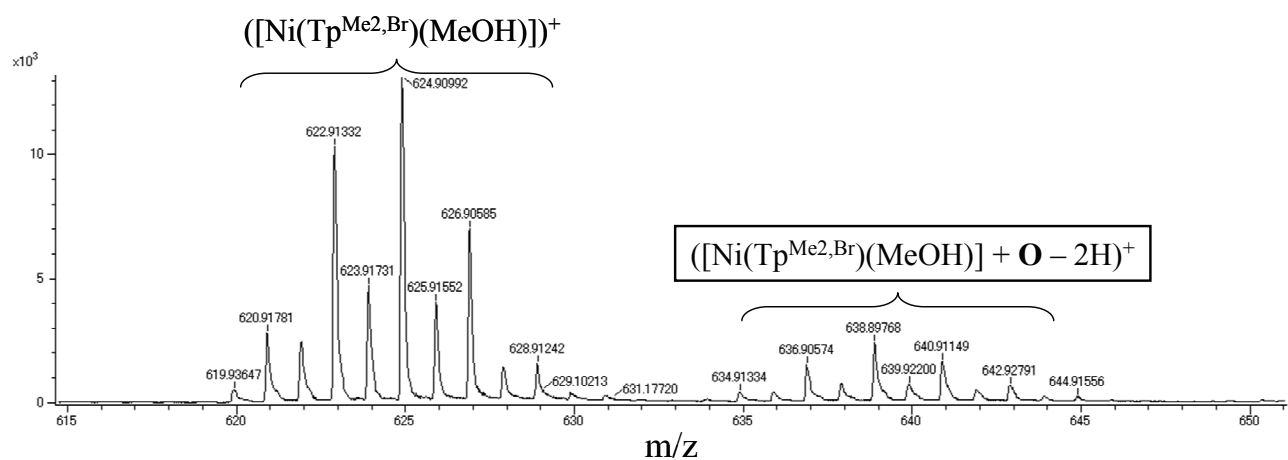


Fig. S9 ESI-MS spectrum of the decomposed products of 2^{Br} derived from the CD_2Cl_2 solution.

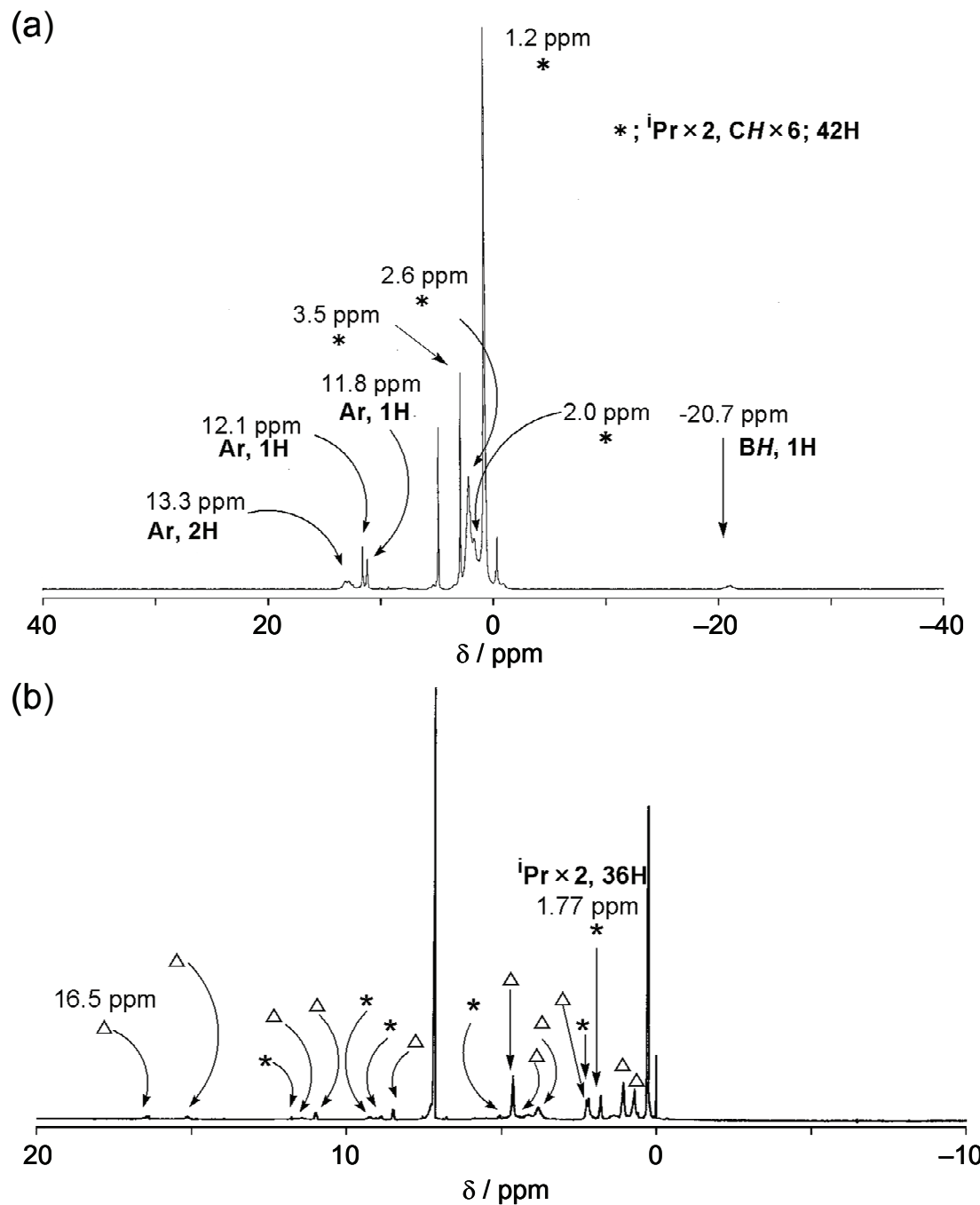


Fig. S10 ^1H NMR spectra of $\mathbf{2}^{\text{Br}}$ and its decomposed products mixture. (a) CD_2Cl_2 solution of $\mathbf{2}^{\text{Br}}$ recorded at 233 K. (b) Decomposed products mixture obtained from Et_2O solution of $\mathbf{2}^{\text{Br}}$ by standing at ambient temperature for one day under Ar and then evaporation. The spectrum was recorded at room temperature in C_6D_6 . Marked signals denote the protons of $\mathbf{4}^{\text{Br}}$ (*) and $\mathbf{5}^{\text{Br}}$ (Δ), respectively.

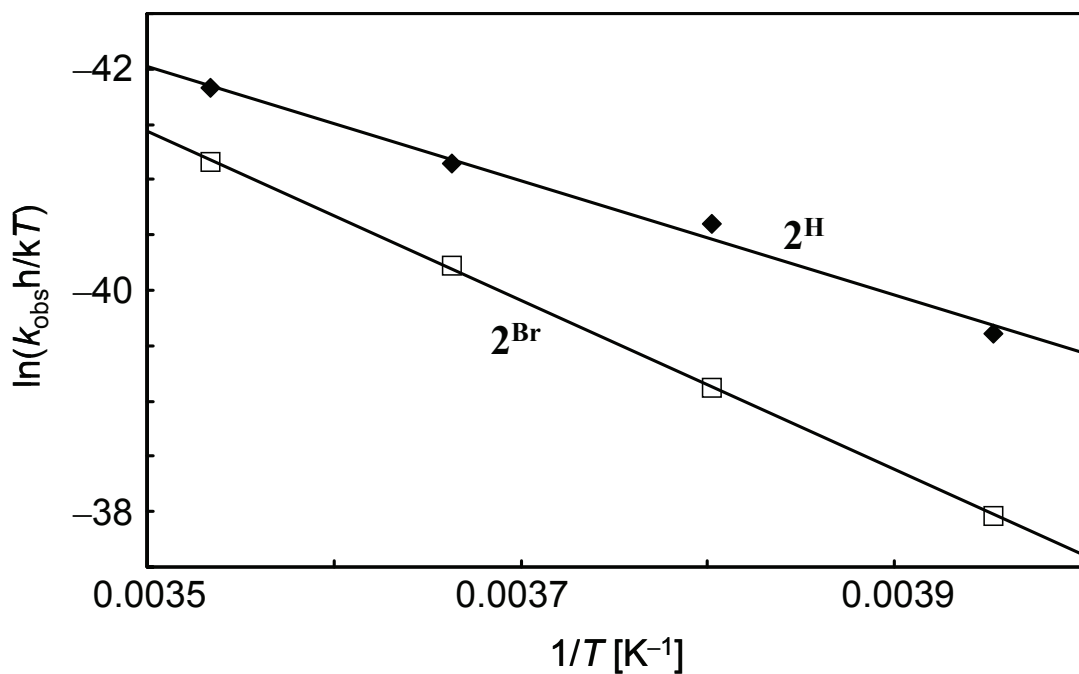


Fig. S11 Eyring plots for the thermolysis of 2^{X} in CH_2Cl_2 .

Table S5 Activation parameters the thermolysis of 2^{X} in CH_2Cl_2 .

Activation parameters	2^{H}	2^{Br}
$\Delta H^{\ddagger} / \text{kcal}\cdot\text{mol}^{-1}$	10.2(7)	15.2(2)
$\Delta S^{\ddagger} / \text{e.u.}$	-31.6(28)	-15.6(7)
$E_a / \text{kcal}\cdot\text{mol}^{-1}$	10.8(7)	15.7(2)
$\ln A$	14.4(14)	22.5(4)